# Effect of Anisotropy on the Ion-Temperature-Gradient Instability

O. Mathey and A. K. Sen

*Department of Applied Physics and Nuclear Engineering, Columbia University, New York, New York 10027*

(Received 21 July 1988)

It is shown that anisotropy in gradient has a substantial effect on the ion-temperature-gradient–driven mode. A gradient in the parallel temperature is needed for an instability to occur, and a gradient in the perpendicular temperature can either enhance or diminish the instability. The latter may be the basis for a stabilization scheme for this mode in tokamaks via strong and appropriate ion-cyclotron-resonance heating. The physical reason for this important role difference is also presented.

PACS numbers: 52.35.Qz, 52.25.Dg, 52.35.Fp, 52.35.Kt

Recent theoretical work[1,2] on the temperature-gradient–driven instability[3,4] has indicated that this mode may be responsible for anomalous ion energy transport across the field lines, making the understanding of the mode all the more crucial to controlled fusion devices. Some experimental evidence of this instability in the TEXT tokamak has also been reported.[5] However, so far no difference has been discussed between the respective roles of the gradients in parallel and perpendicular ion temperatures $T_{i\parallel}$ and $T_{i\perp}$. We show that the roles of $\eta_{i\parallel} \equiv d\ln T_{i\parallel}/d\ln n_0$ and $\eta_{i\perp} \equiv d\ln T_{i\perp}/d\ln n_0$ are profoundly different, where $n_0$ is the density. Because the ions are strongly ion-cyclotron-resonance heated in some machines of interest, perpendicular ion temperatures will typically be far greater than the parallel ones and the corresponding gradients can be quite different. We will consider a shearless slab geometry at low $\beta$ which allows us to write the magnetic field as $\mathbf{B} = B_0\mathbf{z} = \text{const}$. Temperature and density gradients are in the $x$ direction. We consider a local analysis at the point of maximum density gradient and write the perturbed potential $\phi$ as $\phi = \phi\exp(ik_\perp y + ik_\parallel z - i\omega t)$, with $k_\perp = m/r_n$, where $m$ is the azimuthal mode number and $r_n$ is the plasma size.

*Dispersion relation.*— Since the mode frequency $\omega \approx k_\parallel v_{\text{th}i}$, with $v_{\text{th}i}$ the parallel ion thermal velocity, the electrons will respond adiabatically,

$$n_e = n_0 e\phi/T_e ,$$

and the ion density response is determined by the method of characteristics.[6] We shall consider a local analysis and assume the mode to be located at the point of maximum gradient and ignore any $x$ dependence. As a zeroth-order distribution function, we will choose the standard Maxwellian solution to the Vlasov equation representing a plasma with finite density and temperature gradients,[6] namely

$$f_0(v_\perp^2, v_\parallel^2, x + v_y/\Omega) = n_0[1 + (-\epsilon + \delta_\perp m v_\perp^2/2k_B T_\perp + \delta_\parallel m v_\parallel^2/2k_B T_\parallel)(x + v_y/\Omega)] \times [m/2\pi T_\parallel]^{1/2}[m/2\pi T_\perp]\exp[-m v_\parallel^2/2k_B T_\parallel - m v_\perp^2/2k_B T_\perp] , \quad (1)$$

where $x$ is measured from the point of maximum gradient and $\delta_\parallel \equiv T_\parallel'/T$, $\delta_\perp \equiv T_\perp'/T$ at the point of maximum gradient. $\Omega$ is the cyclotron frequency. We shall write $L_n \equiv n/n'$ at the point of maximum gradient, and $\epsilon$ is such that $L_n^{-1} = -\epsilon + \delta_\perp + \delta_\parallel/2$. Poisson's equation will then lead to

$$1 + \tau_\perp + S_0(\tau_\parallel - \tau_\perp) + k_\perp^2\lambda_D^2 + S_0\tau_\parallel \xi Z(\xi) + \xi^* S_0[Z(\xi) + \eta_{i\parallel}\xi + \eta_{i\parallel}(\xi^2 - \tfrac{1}{2})Z(\xi) - \eta_{i\perp} bGZ(\xi)] = 0 . \quad (2)$$

In the above equation $\xi \equiv \xi_i \equiv \omega/k_\parallel v_{\text{th}i}$, $\tau_\perp \equiv T_e/T_{i\perp}$, $\tau_\parallel \equiv T_e/T_{i\parallel}$, $b \equiv k_\perp^2\rho_i^2$, where $\rho_i$ is the ion Larmor radius, $S_0 \equiv e^{-b}I_0(b)$, $G \equiv 1 - I_1(b)/I_0(b)$, where the $I$'s are the usual modified Bessel functions, $\lambda_D$ is the electron Debye length, $\xi^* \equiv \omega_e^*/k_\parallel v_{\text{th}i}$, where $\omega_e^*$ is the electron diamagnetic frequency, and $Z$ is the plasma dispersion function. We will also write $\xi_r$ as the real part of $\xi$, and $\omega_r$ as the real part of the frequency $\omega$.

*Marginal stability analysis.*— We now determine the values of $\eta_{i\parallel}$ and $\eta_{i\perp}$ that are such that $\gamma = \text{Im}(\omega) = 0$. If $\omega$ is real, the factor multiplying $Z(\xi)$ is real and must be zero since $Z(\xi)$ is complex for a real argument. This leads to the condition

$$\eta_{i\parallel}\xi^*\xi^2 + \tau_\parallel\xi + \xi^*(1 - \eta_{i\parallel}/2 - \eta_{i\perp} bG) = 0 . \quad (3)$$

The dispersion relation then becomes

$$\xi\xi^* S_0\eta_{i\parallel} + 1 + \tau_\perp + S_0(\tau_\parallel - \tau_\perp) + k_\perp^2\lambda_D^2 = 0 . \quad (4)$$

From Eqs. (3) and (4), an instability will arise for a given $\eta_{i\parallel}$ when

$$\eta_{i\perp} > \{[1 + \tau_\perp + S_0(\tau_\parallel - \tau_\perp) + k_\perp^2\lambda_D^2]^2/\xi^{*2}S_0^2\eta_\parallel bG\} - \{[1 + \tau_\perp + S_0(\tau_\parallel - \tau_\perp) + k_\perp^2\lambda_D^2]/\xi^{*2}S_0\eta_\parallel bG\} + (1 - \tfrac{1}{2}\eta_{i\parallel})/bG . \quad (5)$$

 

Conversely, for a given $\eta_{i\perp}$, an instability will arise when

$$\eta_{i\parallel} > 1 - \eta_{i\perp}bG + \left[(1-\eta_{i\perp}bG)^2 + 2[1+\tau_\perp+S_0(\tau_\parallel-\tau_\perp)+k_\perp^2\lambda_D^2]\{[1+\tau_\perp+S_0(\tau_\parallel-\tau_\perp)+k_\perp^2\lambda_D^2]-S_0\}/\xi^{*2}S_0^2\right]^{1/2}. \quad (6)$$

It is clear from Eq. (5) that $\gamma=0$ is impossible when $\eta_{i\parallel}=0$, but this is quite possible even when $\eta_{i\perp}=0$ according to Eq. (6). Moreover, in the limit $\xi_r \gg 1$, $\gamma \ll \omega_r$, we obtain ($\tau_\parallel = 1$)

$$\xi_r = S_0\xi^*(1-bG\eta_{i\perp})/[1+\tau_\perp(1-S_0)+k_\perp^2\lambda_D^2], \quad (7)$$

$$\gamma/k_\parallel v_{\mathrm{th}i} = \pi^{1/2}\xi_r^2\exp(-\xi_r^2)[\xi_r/\xi^* + 1 - bG\eta_{i\perp} - \tfrac{1}{2}\eta_{i\parallel} + \eta_{i\parallel}\xi_r^2]/(bG\eta_{i\perp}-1). \quad (8)$$

When $\eta_{i\parallel}=0$, Eq. (8) always yields $\gamma<0$. Consequently, when $\eta_{i\parallel}=0$ an instability is ruled out for all $\eta_{i\perp}$, since an infinite $\eta_{i\perp}$ would be required to reverse the sign of $\gamma$, as per Eq. (5).

Typical results are depicted in Fig. 1 for $k_\parallel L_n = 0.1$. Instead of the customary marginal stability ($\gamma=0$) diagram, we plot $\eta_{i\parallel}$ vs $\eta_{i\perp}$ for a low growth rate of $\gamma/(k_\parallel v_{\mathrm{th}i}) = 0.07$ ($\gamma/\omega_r \approx 0.03$), which may be closer to a more meaningful threshold for experimental observation of the instability. One can see that for a typical mode, say $b=1$, increasing $\eta_{i\perp}$ from 0 will be at first very destabilizing, and then very stabilizing. The other two curves in Fig. 1 show the minimum $\eta_{i\parallel}$ for all possible $b$'s for two sets of values for the temperature ratios $\tau_\parallel$ and $\tau_\perp$. It is noted that $\eta_{i\parallel}$ reaches a minimum for some $\eta_{i\perp}$ in both cases, after which an increase in $\eta_{i\perp}$ will actually be stabilizing for all modes. We also note the stabilizing affect of lower temperature ratios $\tau_\parallel$ and $\tau_\perp$.

In Fig. 2, we show the result for the case of a flat density profile ($L_n \to \infty$). We again note the similar features of a minimum value for $\delta_\parallel$ for some $\delta_\perp$, for a given $k_\parallel$, and the stabilizing affect of increasing $\delta_\perp$ beyond that value for all modes, as well as that due to lower temperature ratios. The stabilizing role of $\eta_{i\perp}$ and $\delta_\perp$ depicted in Figs. 1 and 2, respectively, may be exploited to stabilize the instability in a tokamak via strong ion-cyclotron-resonance heating with appropriate heating profile. We will now proceed to explain the physical mechanism of the instability and the different roles of $\eta_{i\perp}$ and $\eta_{i\parallel}$.

*Physics of the mode*, $\eta_{i\perp,\parallel}=0$.— When no ion temperature gradient is present, Eqs. (7) and (8) yield a stable, electron-drift mode. The physical reason for stability is explained via Fig. 3. Since $\xi_e = \omega/k_\parallel v_{\mathrm{th}e} \ll 1$ and $\xi_i \approx 1$, we are far away from electron resonance but close to ion resonance. In region 3(a), the resonant ions are moved by the $\mathbf{E}\times\mathbf{B}$ drift from a zone of high density into the midplane, whereas in 3(b), ions are moved from a zone of low density into the same midplane. Ions are accelerated in 3(a) and decelerated in 3(b). But since the density at the midplane is higher in 3(a) than in 3(b), the result is a net energy drain from the wave resulting in its damping. This density difference is $\propto \partial f_0/\partial x$. This is a configuration-space-induced phenomenon.

In this regime, ion waves are well known to be strongly damped,[6] and our numerical results verify this fact. Density-gradient effects are more than compensated for by Landau damping. We will shortly review the physical reason for this stabilization.

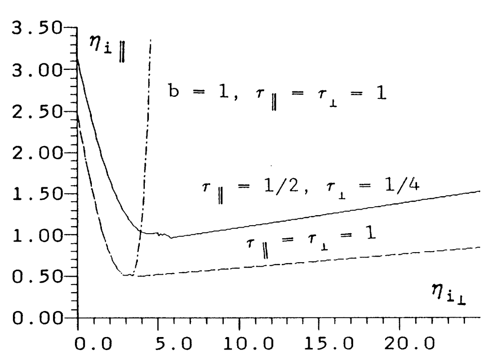


FIG. 1. Experimentally meaningful (small $\gamma/k_\parallel v_{\mathrm{th}i} \approx 0.07$) marginal stability diagram in $\eta_{i\parallel}$-$\eta_{i\perp}$ plane for $k_\parallel L_n = 0.1$. The first curve shown is for $b=1$, $\tau_\parallel \equiv T_e/T_{i\parallel} = \tau_\perp \equiv T_e/T_{i\perp} = 1$. The region above the curve is experimentally unstable and that below is stable. The second curve is for $\tau_\parallel = \frac{1}{2}$, $\tau_\perp = \frac{1}{4}$. The region above it is experimentally unstable for some $b$ and that below is stable for all $b$. The third curve is for $\tau_\parallel = \tau_\perp = 1$. Again, the region below the curve is stable for all $b$, and that above is unstable for some $b$.

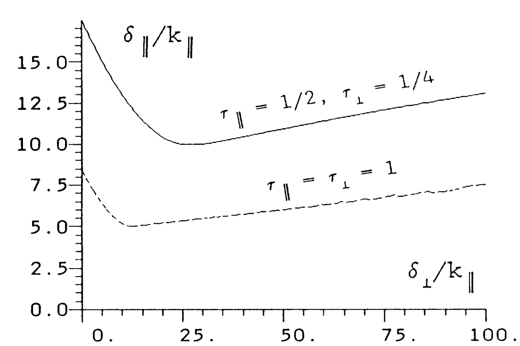


FIG. 2. Experimentally meaningful (small $\gamma/k_\parallel v_{\mathrm{th}i} \approx 0.07$) marginal stability diagram in $\delta_\parallel$-$\delta_\perp$ plane for a flat density profile ($L_n \to \infty$). $\delta_\parallel$ and $\delta_\perp$ are the inverse ion-temperature-gradient scale lengths of $T_{i\parallel}$ and $T_{i\perp}$. The region above a particular curve is experimentally unstable for some $b$ and that below is stable for all $b$. The curves shown are for $\tau_\parallel \equiv T_e/T_{i\parallel} = \tau_\perp \equiv T_e/T_{i\perp} = 1$ and $\tau_\parallel = \frac{1}{2}$, $\tau_\perp = \frac{1}{4}$.

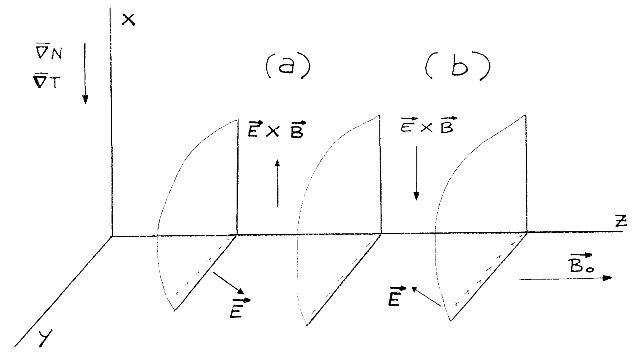


FIG. 3. The physics of the mode.

*Physics of the mode,* $\eta_{i\parallel,\perp}\neq 0$.—When $\eta_{i\parallel,\perp}\neq 0$, the electron wave will be further damped by the $x$-space mechanism described above, since the net effect of the temperature gradient will be to increase $\partial f_0/\partial x$ as a result of the additional gradient in temperature and hence the density difference between zones 3(a) and 3(b).

In regard to the ion wave, as $\eta_i$ increases, parallel compression of the plasma will be more and more coupled to perpendicular motion through ion pressure changes in $\mathbf{E}\times\mathbf{B}$ motion, resulting in the excitation of the ion waves that were originally Landau damped. These ion waves have a real frequency of the opposite sign of that of the electron wave, and therefore have an opposite direction of $\mathbf{E}\times\mathbf{B}$ motion since $\delta x_{\mathbf{E}\times\mathbf{B}}\propto E/B\omega$. The ions in Fig. 3(a) now do work against the wave, while ions in 3(b) gain energy from the wave, in strict analogy to the role of the electrons in the collisionless drift instability. But since region 3(a) has more particles, and since $\partial f_0/\partial x$ is steeper than with only a density gradient present, there is now enough net energy into the wave to overcome Landau damping and produce an instability for adequate values of $\eta_i$ and $\xi$.

A rough estimate of $\gamma$ can be arrived at easily. The resonant ions will have $v_\parallel \approx \omega_r/k_\parallel$, and their displacement along the $x$ axis is $\delta x = [cE_\perp(b)/B]t$. We note that the $\mathbf{E}\times\mathbf{B}$ effect depends strongly on the finite-Larmor-radius effect, and therefore we write $E(b)$. It actually turns out that $E(b)\approx E_\perp S_0(b)$. The number of such ions per unit volume is $f_0(v_\parallel=\omega_r/k_\parallel, x, T(x))\Delta v_\parallel$, where $\Delta v_\parallel$ is the velocity spread near resonance. One may estimate that the ions remain resonant within half a wavelength of the peak, so that $t\Delta v_\parallel \approx \lambda_\parallel/2=\pi/k_\parallel$. The excess resonant ion density [Fig. 3(a)–Fig. 3(b)] is then

$$\delta n_{\rm res} = -\delta x(\partial/\partial x) f_0(\omega_r/k_\parallel, x, T(x))\Delta v_\parallel .$$

From the definition of $f_0$ in Eq. (1) we obtain

$$\partial f_0/\partial x = n_0[-\epsilon+\delta_\perp m v_\perp^2/2k_BT_\perp+\delta_\parallel m v_\parallel^2/2k_BT_\parallel] \times [m/2\pi T_\parallel]^{1/2}[m/2\pi T_\perp]\exp[-mv_\parallel^2/2k_BT_\parallel - mv_\perp^2/2k_BT_\perp]. \quad (9)$$

We may take $mv_\perp^2\approx 2k_BT_\perp$, and write $\epsilon=-L_n^{-1}+\delta_\perp+\delta_\parallel/2$. We also have $v_\parallel\approx\omega_r/k_\parallel$. $\delta n_{\rm res}$ will then become

$$\delta n_{\rm res} = -[n_0cE_\perp S_0(b)\pi/Bk_\parallel][L_n^{-1}+\delta_\parallel(m\omega_r^2/2k_Bk_\parallel^2T_\parallel-\tfrac{1}{2})] \times [m/2\pi T_\parallel]^{1/2}[m/2\pi T_\perp]\exp[-mv_\parallel^2/2k_BT_\parallel - mv_\perp^2/2k_BT_\perp]. \quad (10)$$

It appears from the above equation that $\eta_{i\perp}$ will not contribute directly to the resonant density, and hence to the power supplied by the particles to the wave. However, $\eta_{i\perp}$ will contribute indirectly through its effect on the real frequency $\omega_r$, as according to Eq. (7), $\omega_r\propto\eta_{i\perp}$ for sufficiently large $\eta_{i\perp}$.

The net power delivered to the wave will be the balance of power input into the wave and Landau power loss. The net power delivered to the wave is $P_{D\eta_i}=eE_\parallel\delta n_{\rm res}\omega_r/k_\parallel$, which can be written with the help of Eq. (10) as

$$P_{D\eta_i} = -[n_0ecE_\parallel E_\perp S_0(b)\pi\omega_r/Bk_\parallel^2][L_n^{-1}+\delta_\parallel(m\omega_r^2/2k_Bk_\parallel^2T_\parallel-\tfrac{1}{2})] \times [m/2\pi T_\parallel]^{1/2}[m/2\pi T_\perp]\exp[-mv_\parallel^2/2k_BT_\parallel - mv_\perp^2/2k_BT_\perp]. \quad (11)$$

The power loss by Landau damping is $(-\omega_r>\gamma)$

$$P_{\rm LD} = -(ec\pi E_\parallel^2\omega_r/mk_\parallel^2)(\partial f_0/\partial v_\parallel) = c(eE_\parallel\omega_r)^2 f_0/k_\parallel^3 T_\parallel . \quad (12)$$

We infer from Eqs. (11) and (12) that

$$P_{\eta_i}/P_{\rm LD}\approx S_0\pi(\omega^*/\omega_r),\quad \xi\ll 1, \quad (13)$$

$$P_{\eta_i}/P_{\rm LD}\approx 2k_\perp\omega_r S_0(b)\pi\delta_\parallel/k_\parallel^2\Omega_i,\quad \xi>\tfrac{1}{2}. \quad (14)$$

These results can be used to elucidate the different roles of $\eta_{i\parallel}$ and $\eta_{i\perp}$. With no $\eta_{i\parallel}$ present, the only term doing work into the wave in Eq. (11) is the $L_n^{-1}$ term. But since $\omega_r\propto\omega^*$, increasing $L_n^{-1}$ will not change the ratio $P_{\eta_i}/P_{\rm LD}$ appreciably in Eq. (13). If, on the other hand, we strongly increase $\eta_{i\perp}$, $\omega_r$ will increase according to Eq. (7), which actually favors Landau damping. Increasing $\eta_{i\perp}$ further with $\eta_{i\parallel}\doteq 0$ will make $|\xi_r|\gg 1$ and result in the depletion of resonant particles and stabilization of the mode. Interestingly, raising $\eta_{i\perp}$ for a given $\eta_{i\parallel}$ will be destabilizing insofar as one moves closer to resonance as $\omega_r$ increases. Increasing $\eta_{i\perp}$ beyond the resonance zone results in a spectacular crash of the growth rate to noise levels for all reasonable $\eta_{i\parallel}$ values,

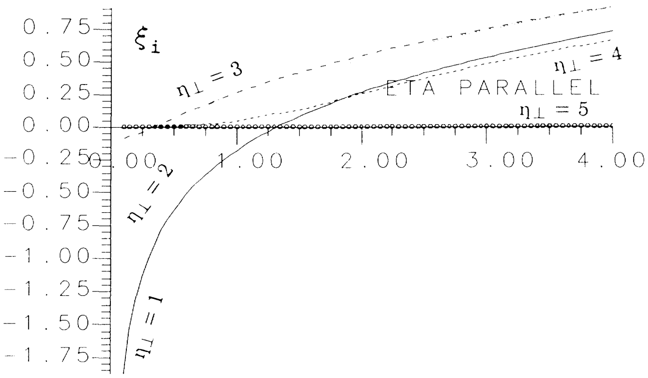


FIG. 4. The value of $\gamma/k_{\parallel}v_{\mathrm{th}i}$ for different $\eta_{i\perp}$ as a function of $\eta_{i\parallel}$. The parameters are $k_{\parallel}L_n=0.1$, $b=1$, $\tau_{\parallel}=\tau_{\perp}=1$.

as Fig. 4 indicates, which depicts the growth rates $\gamma/k_{\parallel}v_{\mathrm{th}i}$ vs $\eta_{i\parallel}$. With our parameters, $b=1$, $\tau_{\parallel}=\tau_{\perp}=1$, and $k_{\parallel}L_n=0.1$, the instability is strongest for $\eta_{i\perp}=3$, and it is completely stabilized at $\eta_{i\perp}=5$, for all $\eta_{i\parallel}$'s $<4$.

After completion of the present work, it was brought to our attention that an independent study of the same topic was being submitted for publication.[7] As in the present study, the author finds that $\eta_{i\parallel}$ is critical for instability. He also concludes that $\eta_{i\perp}$ is stabilizing, whereas our results indicate that this is the case at high $\eta_{i\perp}$ only. $\eta_{i\perp}$ can be very destabilizing indeed below resonance as Fig. 4 indicates. There also appears to be an ambiguity between the roles of anisotropic temperature (whose role is minor) and anisotropic temperature gradient (whose role is critical).

This research was supported by Department of Energy Grant No. DE-FG02-87ER 53257. The authors are also grateful for several very fruitful discussions with S. Migliuolo.

[1]S. M. Wolfe, M. Greenwald, R. Gandy, R. Granetz, C. Gomez, D. Gwinn, B. Lipschultz, S. McCool, E. Marmar, J. Parker, R. R. Parker, and J. Rice, Nucl. Fusion **26**, 329 (1986).

[2]R. J. Groebner, W. Pfeiffer, F. P. Blau, K. H. Burell, E. S. Fairbanks, R. P. Seraydarian, H. St. John, and R. E. Stockdale, Nucl. Fusion **26**, 543 (1986).

[3]T. Antonsen, B. Coppi, and R. Englade, Nucl. Fusion **19**, 641 (1979).

[4]S. Migliuolo, Phys. Fluids **28**, 2778 (1985).

[5]D. Brower *et al.*, Phys. Rev. Lett. **59**, 48 (1987).

[6]K. Miyamoto, *Plasma Physics for Nuclear Fusion* (MIT Press, Cambridge, MA, 1980).

[7]S. Migliuolo, Phys. Lett. A (to be published).